Advances in Environmental Technology 12(3) 2026, 407-419.

Iranian Reasearch Organization for Science and Technology (IROST)

Advances in Environmental Technology

Journal home page: https://aet.irost.ir

Removal of copper (II) ion by functionalized graphene oxide nano adsorbent from wastewater sample

Iman Khonsha*

Department of Chemical Engineering, Shi.C., Islamic Azad University, Shiraz, Iran

ARTICLE INFO

Document Type:
Research Paper

Article history:
Received 03 May 2025
Received in revised form
10 June 2026
Accepted 13 June 2026

Keywords:
Functionalized graphene oxide
Adsorption isotherm
Copper ion

ABSTRACT

In the present research, a magnetic nanostructure based on graphene oxide and iron oxide modified by the amino acid tryptophan was synthesized. The properties of the adsorber were determined using a Fourier transform infrared spectrometer, elemental analysis, X-ray diffraction, a scanning electron microscope, and a vibrating-sample magnetometer. Optimum parameters such as pH, contact time, amount of used adsorbent, initial concentration of copper ions, and the effect of temperature were investigated. Adsorption isotherm studies were conducted using the Langmuir and the Freundlich models, and the Langmuir isotherm model was found to be more consistent with the adsorption process. The theoretical maximum adsorption capacity of the adsorbent was 125 mg of copper per gram of adsorbent, which was close to the maximum adsorption capacity of the adsorbent in the real state (118 mg of copper per gram of adsorbent). To investigate the thermodynamics of adsorption, the Van't Hoff Equations were used. The results indicated that the adsorption process was endothermic. In addition, the removal rate of copper ions from the real wastewater sample in the presence of other ions was determined to be 46%.

1. Introduction

Metals are widely used across various industries, making them one of the most common sources of water pollution [1]. Heavy metals such as copper, zinc, cadmium, lead, nickel, and mercury are present in water systems. These elements can be transferred to living beings and ultimately to humans through various ecosystems. Long-term contact with even small amounts of these elements can cause poisoning. The reason for this is the lack of destruction and metabolism of these toxic substances in the body [2]. Among the most significant catastrophes of heavy metal pollution is the epidemic of Minamata disease in Japan [3]. Also, water pollution in the Persian Gulf is a national example of the serious threat from heavy metals. This is more than 47 times the international average, turning this ecosystem into one of the most polluted marine areas in the world [4]. Therefore, various methods have been used to reduce and remove metal ions from water sources.

*Corresponding author Tel.: +98 7136410043
E-mail: iman.khonsha@iau.ac.ir
DOI: 10.22104/aet.2026.7599.2132

In this regard, using surface adsorption [5], reverse osmosis [6], solvent extraction [7], precipitation [8], ion exchange [9], and electrochemical cells [10] are among the most common methods for separating heavy metals from polluted water.

Surface adsorption, which belongs to the category of physical-biological methods, is a cost-effective method with high efficiency [11]. The surface adsorption method is utilized to remove heavy metals using different adsorbents. The use of nanoparticles as adsorbents has been expanded with the advancement of nanotechnology. Nanomaterials behave differently from macrostructure or microstructure materials, which is due to their small size, high specific surface area, crystalline structure, and high reactivity [12]. In a new study, the superior effectiveness of graphene derivatives compared to conventional adsorbents, such as activated carbon, was investigated, particularly in the field of heavy metals, dyes, pharmaceuticals, and emerging pollutants [13]. In another recent study, a phosphorus-doped 3D graphene oxide was used to remove imipramine from wastewater, and the effect of individual factors on imipramine adsorption was investigated with batch experiments [14].

In this research work, magnetic graphene oxide nanoparticles modified by tryptophan were synthesized and studied in order to remove heavy metals from wastewater. Due to the magnetic properties of graphene oxide in the synthesized adsorbent, it could be easily removed from the wastewater by creating a magnetic field. Therefore, this adsorbent was environmentally safe. The previously mentioned nanostructures were synthesized in three successive stages in such a way that, at first, the graphene oxide nanoparticles were synthesized from the graphite precursor by Hammer's method. Then, iron (II) and (III) chlorides were deposited on the surface of graphene oxide nanoparticles and became a magnetic product by the co-precipitation method. Finally, the surface modification of magnetic graphene oxide nanoparticles was performed using tryptophan amino acid. In the following, the separation process of copper metal ions from aqueous samples was studied via the surface adsorption method using the existing modified nanoparticle. Adsorption kinetics studies for this adsorbent have been previously published in a similar study [15].

2. Materials and methods

2.1. Reagents, solutions and instrumentation

All the materials used were of high purity and without further concentration and purification. The graphite powder, sodium nitrate, potassium permanganate, aqueous iron (II) and (III) chloride, tryptophan powder, copper sulfate, sulfuric acid, hydrochloric acid, ammonia, nitrogen gas, acetic acid, and nitric acid were purchased from Merck.

The pH was adjusted using a Metrohm 728 pH meter. Spectrum Two Fourier-transform infrared spectrometer (FTIR), manufactured by PerkinElmer Company, was used to investigate the surface modification process of the nanoparticles. Phase identification and investigation of the crystal structure of synthesized nanoparticles were performed using the X Pert Pro X-ray Diffractometer manufactured by the Panalytical Company.

A SIGMA VP field emission scanning electron microscope manufactured by the Zeiss Company was utilized to image the synthesized nanoparticles. The measurement of heavy metal concentration in the solutions was carried out by a PerkinElmer AAnalyst 800 atomic adsorption spectrometer using the hollow-cathode lamp corresponding to the desired ion and at the desired wavelength, with an air-acetylene flame. In this regard, the concentration of the samples was determined using the standard curve. A 2-Tesla neodymium-iron-boron magnet (Iran Magnet Company) was used to separate nanoparticles from the solution. The Vibrating-Sample Magnetometer (VSM) analysis device, with the technical specifications of the VSM LBKFB device with a maximum applied field of 1.4 Tesla in an air gap of 10 mm, was used to investigate the magnetic properties of nanoparticles. One repetition was used for each experiment.

2.2. Synthesis of Nano-Adsorbent

The adsorbent used in the current research is a nanostructure whose surface is modified in 3 stages to optimally adsorb the heavy metal copper. First, graphene oxide (GO) nanoparticles were

synthesized by the modified Hummer method [16] and then added using the co-precipitation of ferrous and ferric ions in an alkaline environment on the surface of graphene oxide [17]. Subsequently, the magnetic graphene oxide (m-GO) nanoparticles were coated with tryptophan amino acid. The three stages of nano-adsorbent synthesis are now ready.

2.2.1. Synthesis of Graphene Oxide

In this stage, 2 g of graphite powder was added to 50 mL of concentrated sulfuric acid and 2 g of sodium nitrate at 0 °C. The solution was mixed for 2 h at 80 °C, and the mixture was stirred for 24 h at ambient temperature using a magnetic stirrer. Then, while the mixture was strongly stirred, 6 g of potassium permanganate was added to it at a temperature of 15 °C. Stirring was continued at 15 °C until the mixture turned into a brown paste. Then the mixture was diluted by adding deionized water. After that, 10 mL of hydrogen peroxide solution (30% by weight) was slowly added to the mixture. At this stage, the color of the mixture changed to bright yellow. After that, the obtained product was centrifuged and washed several times with hydrochloric acid solution (in the volume ratio of 1:10). Finally, the resulting powder was dried at ambient temperature.

2.2.2. Magnetization of Graphene Oxide

Magnetic nanoparticles were synthesized by the co-precipitation method, with a slight change in the method reported in references. According to this method, 2.33 g of iron (III) chloride and 0.86 g of iron (II) chloride were dissolved in 100 mL of 0.4 M hydrochloric acid solution, and the graphene oxide synthesized in the previous stage was added to it. Then, the mixture was deoxygenated with nitrogen gas. At the same time, 400 mL of 1/4 M solution of ammonia was prepared and deoxygenated with nitrogen gas. After that, the ammonia solution was subjected to ultrasonic waves, and the mixture of iron (II) and (III) was suddenly poured into it while still being degassed. The above mixture was kept under these conditions for 30 minutes. After that, the produced product was separated from the solution using a magnet. Then, the produced m-GO was washed several times with deionized water and finally dried in a vacuum oven at 60 ^{0}C for 12 h.

2.2.3. Modification of Magnetic Graphene Oxide Surface by Tryptophan

Tryptophan was deposited on magnetic graphene oxide plates by the co-precipitation method. In this way, at first, 0.5 g of tryptophan powder was slowly added to 100 mL of acetic acid-water solution (5% by volume) and placed in an ultrasonic bath until it was completely dissolved. Then the aforementioned solution was filtered to remove possible impurities. After that, the m-GO synthesized in the previous stage was added to the tryptophan solution. In the next stage, while the solution was under ultrasonic waves, 0.1 M soda solution was added drop by drop until the pH of the solution reached 10. After adjusting the pH to the desired level, the solution was subjected to ultrasonic waves with an intensity of 100 W for 2 h and then mechanically stirred for half a day at a temperature of 60 °C. In the final stage, the adsorbent particles (m-GO & Tryp) were filtered and washed several times using ethanol and deionized water. Finally, the solution was dried in an oven under vacuum and at low temperature and was powdered by a mill. Figure 1 represents a schematic of magnetic graphene oxide modified with tryptophan.

2.3. Analysis of Isotherm

In this research, all adsorption experiments were performed in a discontinuous system. CuSO4. 5H2O was used to make a mother solution of 1000 mg/liter of copper metal, and other solutions with specific concentrations were made from the mother solution. The experiments were carried out at ambient temperature in a 50-mL Erlenmeyer flask as a reaction vessel, with two repetitions. The concentration of heavy metals in the samples was determined with a flame atomic adsorption device. First, the effect of surface modification was investigated by performing the adsorption process on the samples of each synthesis stage.

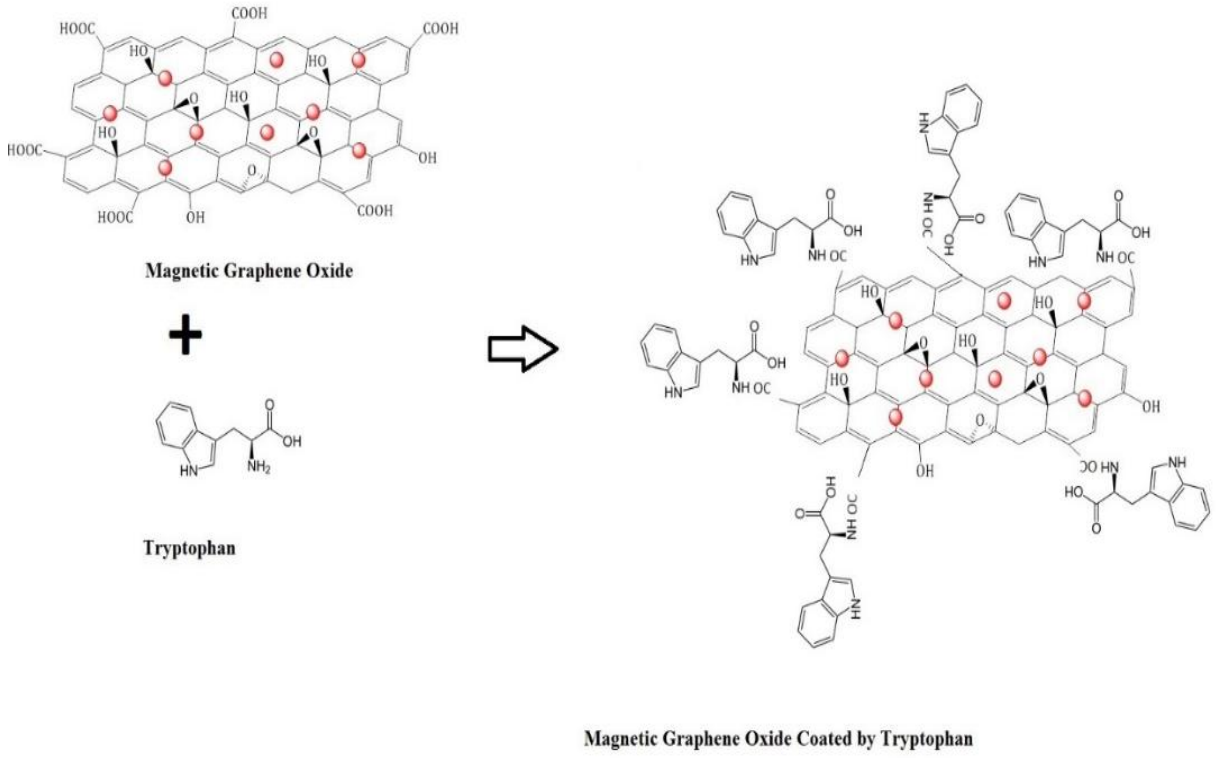

Fig. 1. Schematic of the synthesis of magnetic graphene oxide modified with tryptophan.

Then, the pH parameters of the solution, the amount of used adsorbent, initial concentration, and contact time were checked and optimized.

The adsorption efficiency was calculated from Equation 1, and the adsorption capacity of the adsorbent was calculated from Equation 2 [18]:

$$R(\%) = \frac{C_o - C_e}{C_o} \times 100 \quad (1)$$

$$q_e = (C_o - C_e)\, V/W \quad (2)$$

In the above equations, C_0 is the initial concentration of copper in the solution (mg.L^{-1}), C_e is the equilibrium concentration or concentration of copper in the solution after the adsorption process (mg.L^{-1}), W is the mass of the used adsorbent (mg), V is the volume of solution (mL), q_e is the adsorption capacity of the adsorbent (mg.g^{-1}), and R is the adsorption efficiency (%).

3. Results and discussion

3.1. Adsorbent Characterization

To identify and prove the success of the surface modification process of the synthesized nanostructure, the Fourier transform infrared spectroscopy (FTIR) method was first employed. Figure 2 shows the FTIR analysis results for the three stages of adsorbent synthesis. In the spectrum related to the first stage of the adsorbent synthesis and the formation of graphene oxide, a broad adsorption band can be seen in the region of 11120 cm, which is related to the stretching vibrations of the ether C-O bond. The band in the spectrum corresponding to the third stage is seen more intensely, which is due to the increase in the number of ether bonds due to the binding of tryptophan to graphene. Similarly, the adsorption band in the wave number of 1446 cm^{-1} is related to ν(C=C) vibrations of the aromatic ring of graphene, which appears as a stronger adsorption band at the wave number 1446 cm^{-1} in the spectrum of the third stage due to the formation of the first type of alcohol group by virtue of the binding of tryptophan to graphene and the presence of the C-O bond in it. The other three adsorption bands in the spectrum of the first stage (a) correspond to the strong peaks in the regions of 1384 cm^{-1}, 1637 cm^{-1} and the average peak of the region 2921 cm^{-1}, which are respectively related to the ν(C-O) vibrations of the first type of alcohol group

CH2OH, ν(C=O) of the carboxylic acid group and the stretching vibrations of C-H groups within the molecule in different regions. The appearance of a weak peak in the wave number 486 cm^{-1} and a strong peak in the region of 619 cm^{-1} in the spectrum of the second stage (b) is related to the stretching vibrations of the Fe-O bond. The consecutive adsorption bands in the regions 777 cm^{-1}, 836 cm^{-1}, and 876 cm^{-1} in the spectrum of the third step (c) are related to the out-of-plane bending vibrations of the N-H bond. The peak at 1617 cm^{-1} corresponds to the C=O bond of the amide group. The appearance of the two-branched adsorption band at the wave numbers 3475 cm^{-1} and 3547 cm^{-1} is related to the stretching vibrations of the NH2 group; the peak in the area of 3418 cm^{-1} is related to the ν(-NH) vibrations, which overlapped with the general vibrations of the OH group and appeared as a broad adsorption band, indicating the modification of the adsorbent surface.

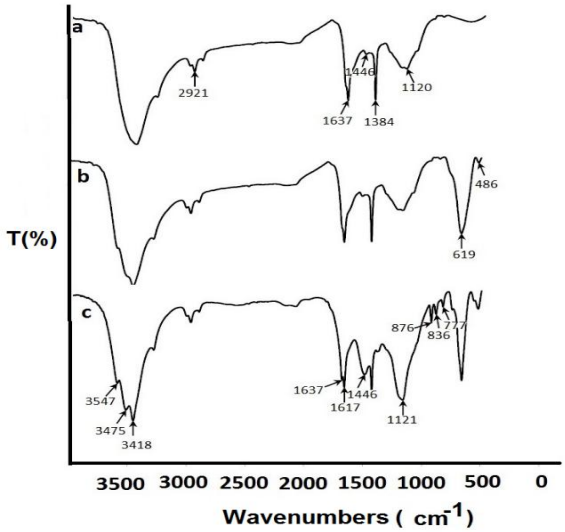

Fig. 2. FTIR analysis for three stages of adsorbent synthesis.

The results of elemental analysis through X-ray Energy Diffraction (EDS) before and after the copper adsorption process are given in Figure 3. Examining the results shows that the synthesized nanostructure has elements of carbon, oxygen, nitrogen, sulfur, and iron in its structure before adsorbing copper, which indicates the presence of carbon chains, oxide groups, amide and thiol functional groups, and magnetic particles in the structure of the particles. Also, the presence of the copper element after the adsorption process confirms good surface adsorption of copper by the m-GO@Tryp complex.

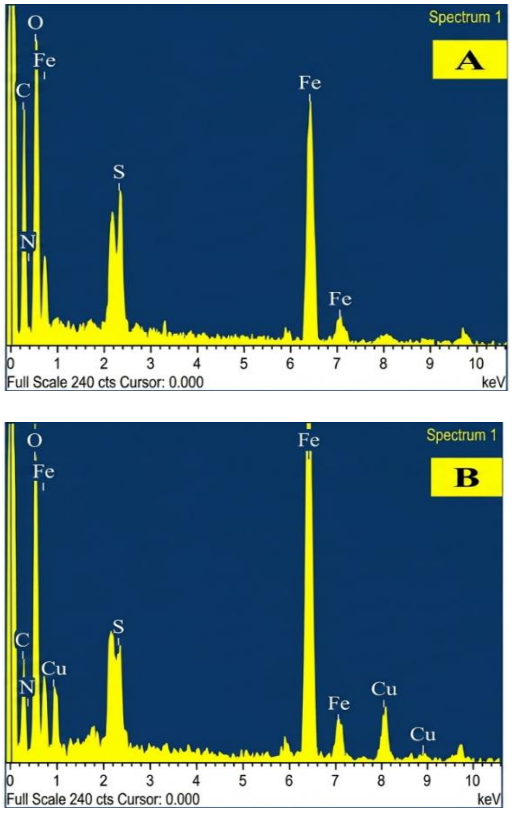

Fig. 3. EDS spectrum of m-GO@Tryp Complex: A) before copper adsorption and B) after copper adsorption.

X-ray diffraction spectrometer (XRD) was used to determine the crystalline or non-crystalline structure of the synthesized adsorbent.

Figure 4 shows the XRD pattern of the modified graphene oxide structure before the copper adsorption process.

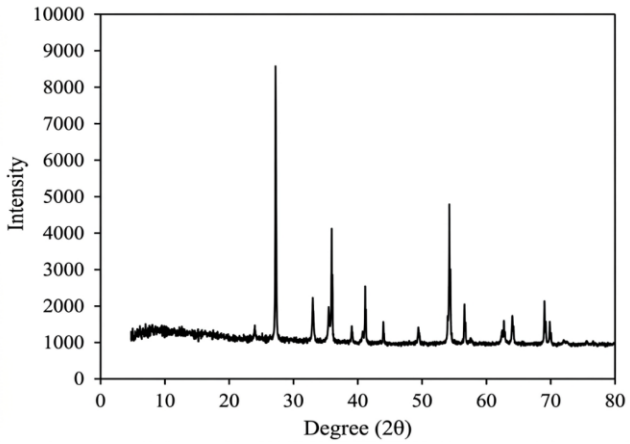

Fig. 4. XRD pattern of the adsorber before adsorption.

According to this model, the synthesized magnetic nanoparticles are single-phase and have a hexagonal orthorhombic crystal system.

In this research, the magnetic properties of nanoparticles were investigated using the Vibrating Magnetometer (VSM) method at ambient temperature. The diagram related to the VSM analysis results of the m-GO@Tryp sample with a saturation magnetization 4.6 emu.g^{-1} is shown in Figure 5.

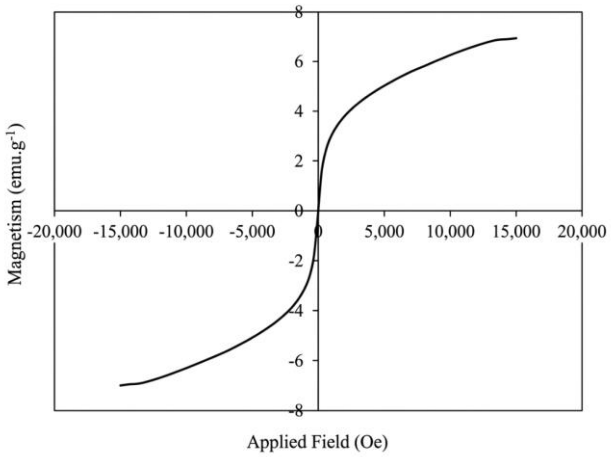

Fig. 5. VSM diagram of m-GO@Tryp nanoparticles.

Figure 6 shows the results of a field emission scanning electron microscope (FESEM). As shown in Figure 6-A, graphene oxide has a two-dimensional sheet structure with appropriate porosity. This structure increases the contact surface of the adsorbent and the pollutant, and subsequently increases the adsorption efficiency. Figure 6-B shows spherical and sometimes asymmetric particles of iron oxide nanoparticles dispersed on the surface of graphene oxide. Figure 6-C is the image of the last stage of surface modification and shows the distribution of tryptophan on the adsorbent surface.

3.2. Investigating the performance of magnetic graphene oxide nanoparticles modified with tryptophan in copper cation adsorption

In order to investigate the effect of the surface modification on the adsorption rate, the percentage of removal of copper ions in the solution was checked using GO, m-GO, and m-GO@Tryp, respectively.

First, a solution of copper cations was prepared, and the desired adsorbent was added to each of the samples. After stirring the solution for 60 minutes at ambient temperature and separating the nanoparticles from the solution using a magnet, the concentration of the solution was measured with an atomic adsorption device; then, the percentage of metal ion removal was calculated according to Equation 1, which is shown in Figure 7.

Examining the figure shows that after each stage of surface modification, the percentage of metal ion removal from the solution increased. Tryptophan has a high metal adsorption capacity due to its amide head (NH_2-), due to the cationic nature of nitrogen and the presence of a lone electron pair. If the surface of magnetic graphene oxide nanoparticles is coated with a thin film of tryptophan, this tryptophan layer greatly contributes to the adsorption of metal cations.

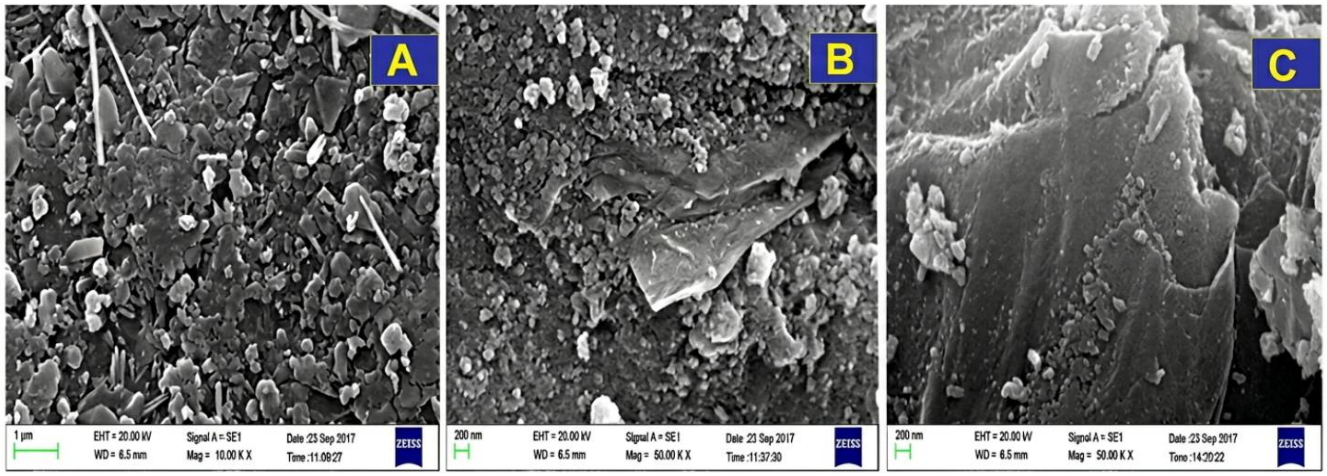

Fig. 6. FESEM image of nanoparticles: A) GO, B) m-GO, and C) m-GO @ Tryp.

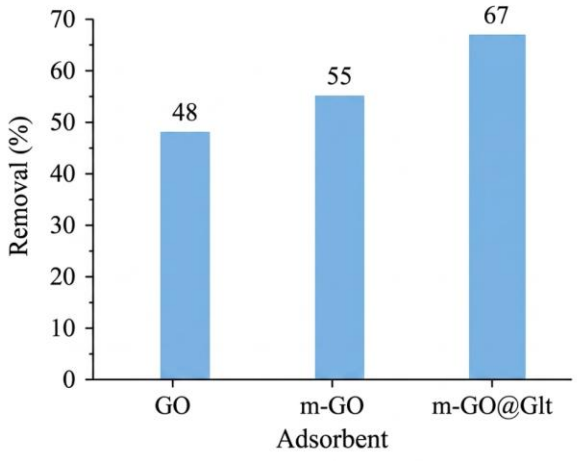

Fig.7. The effect of surface modification on the removal rate of copper ions.

3.3. Optimizing parameters being effective in adsorption

3.3.1. pH of solution

In order to investigate the effect of pH, the adsorption process was performed by adjusting the pH of the samples in values between 2 and 7. Since the pH of the solution was between 5.2 and 5.3, diluted nitric acid was used to lower the pH, and diluted soda was used to increase it. In Figure 8, the adsorption changes are reported according to the pH value.

According to the figure, the maximum amount of adsorption occurred at a pH equal to 5, so pH=5 was chosen as the optimal pH. At pH higher than 6, a decrease in adsorption could be seen, which was due to the formation of divalent copper cations.

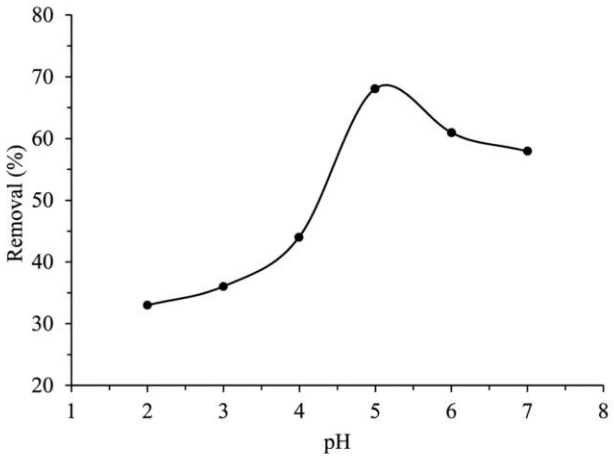

Fig. 8. Effect of pH on adsorption rate.

3.3.2. Investigating the effect of contact time

To check the effect of contact time, only the adsorption time was changed. All other adsorption conditions were fixed, as in previous steps. The results are reported in Figure 9. Investigations show that in the early times, the adsorbent had many active sites; therefore, the increase in time was accompanied by an increase in the chance of copper ions encountering the adsorbent, so adsorption occurred quickly, and the slope of the curve was high. After some time, a major part of the adsorbent surface was filled by the adsorbent, and the available sites became less, so the slope of the curve decreased. This happened after 60 minutes, so 60 minutes was chosen as the optimal time. Finally, the surface of the adsorbent was completely filled with the adsorbent, and through the formation of the internal penetration process, the speed of adsorption became very low; so, the adsorption process had reached equilibrium, and adsorption will no longer occur with the passage of time.

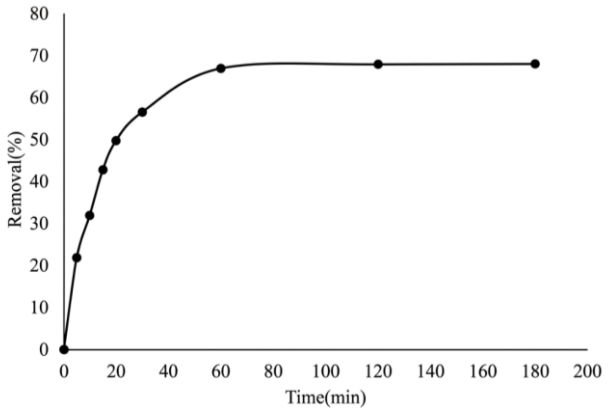

Fig. 9. The effect of contact time on the amount of adsorption.

3.3.3. Checking the amount of adsorbent

In this study, 0.01-0.15 g of adsorbent was added to the copper cation aqueous solution, and after the adsorption process, the concentration of the samples was read by an atomic adsorption device. It can be predicted that as the amount of adsorbent increases, the amount of adsorption also increases, but the purpose of this study is to optimize the amount of used adsorbent. The resulting data in the diagram of Figure 10 show that at a constant concentration, the higher the amount of adsorbent, the adsorption will increase,

until either all the ions in the solution are adsorbed by the adsorbent or the adsorbent is saturated. The curve in the diagram has a great slope up to the amount of 0.1 g of the adsorbent. But from 0.1 to 0.15 g, by doubling the amount of adsorbent used by 1.5%, the amount of adsorption increases by only 1%. Therefore, the value of 0.1 g of the adsorbent was chosen as the optimum amount of adsorbent.

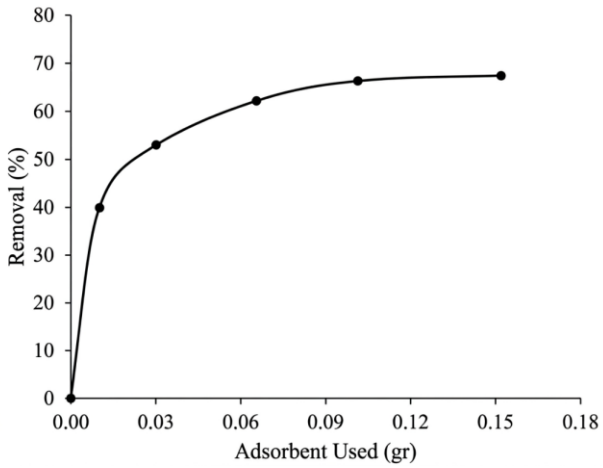

Fig. 10. Evaluation of the effect of the amount of used adsorbent on the amount of copper ion removal.

3.3.4. Investigating the initial concentration of copper cation

To investigate the effect of the initial concentration on the adsorption process of copper ions, a solution sample was prepared with concentrations ranging from 10 to 400 mg/L. After performing the adsorption tests, the concentration of the samples was determined using an atomic adsorption device. In this experiment, because the initial concentration is variable, the removal rate is no longer a suitable parameter to investigate the adsorption process; Therefore, the parameter of adsorption capacity of the adsorbent is introduced and used to examine the effect of the initial concentration using Equation 2 and according to the diagram in Figure 11; the adsorption capacity of the adsorbent for copper metal ions is 118 (mg/g) of the adsorbent.

3.3.5. Investigating the effect of temperature

In order to investigate the effect of temperature on the adsorption process, four samples were placed in environments with temperatures of 0, 25, 40, and 60 °C, and the adsorption process took place. The results are shown in the diagram in Figure 12. By examining the diagram and considering the upward trend of the temperature curve in terms of the amount of removal, it can be concluded that the adsorption process of copper ions by the m-GO@Tryp adsorbent is an endothermic process.

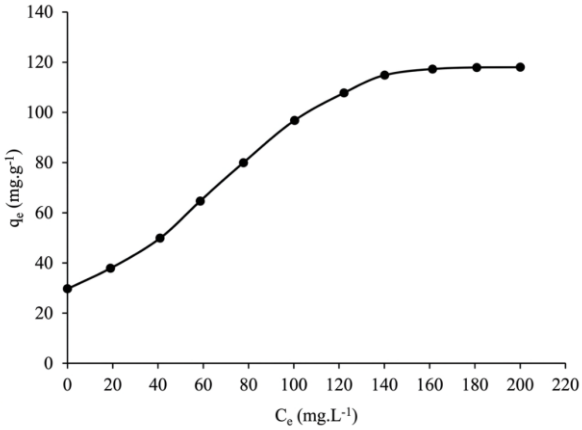

Fig. 11. The effect of the initial concentration of the solution on the adsorption capacity.

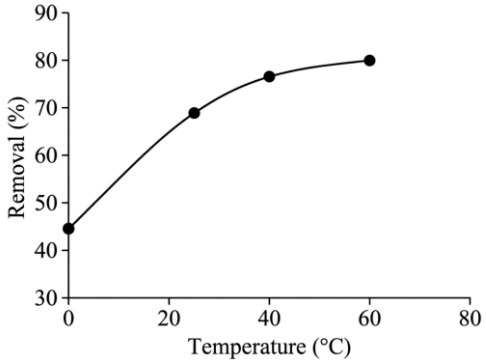

Fig. 12. Effect of temperature on adsorption.

3.3.6. Investigating the adsorbent recovery

In order to investigate the process of adsorbent recovery, an 80ppm copper aqueous solution was first prepared. 40 mL of the solution was poured into a Falcon CC50 tube, and the rest was kept as a control sample. The adsorption operation was carried out under optimal conditions, i.e., solution pH = 5, adsorbent amount = 0.1 g, and contact time = 60 minutes at ambient temperature, by placing the containers on a shaker. Then the nanoparticles were separated by centrifugation and a magnet, and the solution concentration was measured with an atomic absorption spectrometer. After that, 40 mL of 1 M nitric acid solution was added to the adsorbent and sonicated for 3 minutes. Then, it

was centrifuged again, and the nanoparticles were separated with a magnet. The concentration of metal ions in nitric acid was also read with an atomic absorption spectrometer to measure the amount of recovered copper. After that, 40 mL of 80 ppm copper solution was added to the recovered adsorbent, and the above steps were repeated. This was repeated four times to determine the amount of adsorbent recovery.

The recovery results show that when fresh adsorbent is used, the adsorption rate is high (68%) because its sites are fully open and accessible. However, after the first recovery stage, the adsorption rate by the adsorbent decreases to 56%. From the second recovery stage onwards, the adsorption rate decreases further to 14%, and in the third recovery stage, the adsorption rate decreases to 12%. Therefore, it can be concluded that the adsorbent can be used only after one regeneration and, after that, it cannot be recovered by an acid washing method.

3.4. Adsorption process isotherms

The Langmuir and Freundlich isotherms are widely used to fit the data obtained from adsorption experiments and have good accuracy; they will be discussed further.

3.4.1. Langmuir isotherm

The Langmuir equilibrium relationship expresses monolayer and homogeneous adsorption of the adsorbed material, and the adsorption reaction that follows this relationship is called the ideal adsorption reaction. The linear form of the Langmuir model is as follows [19]:

$$\frac{C_e}{q_e} = \frac{1}{q_{max}\, K_L} + \frac{C_e}{q_{max}} \quad (3)$$

The value of C_e was determined by performing the experiment, and the value of q_e was calculated through Equation 2. Figure 13 shows the linear drawing of C_e/q_e in terms of C_e using the Langmuir equation for the adsorption process of copper ions under optimal conditions.

According to the value of the correction coefficient (R^2=0.9078), the Langmuir model shows a high agreement with the data of the adsorption process. The parameters of the Langmuir model for the surface adsorption process of copper ions are given in Table 1.

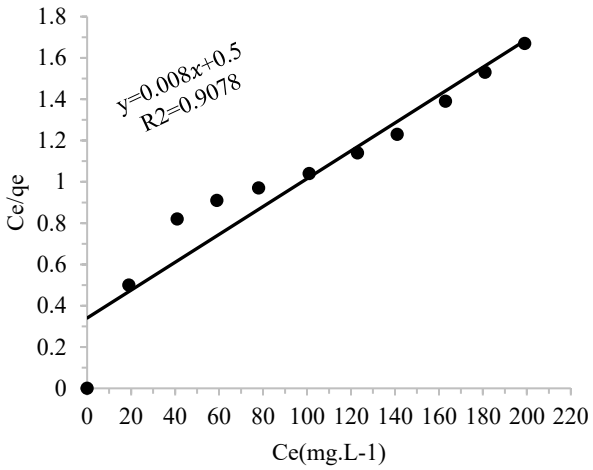

Fig. 13. Langmuir isotherm of copper ion adsorption by the m-GO@Tryp adsorbent.

3.4.2. Freundlich isotherm

The Freundlich isotherm is based on the assumption that the adsorbent has a non-uniform surface consisting of different levels of adsorption sites. The linear form of the Freundlich model is as follows [16]:

$$log(q_e) = log(K_F) + \frac{1}{n} log(C_e) \quad (4)$$

By linearizing and plotting the values of log (q_e) in terms of log (C_e), Freundlich model parameters can be calculated. The adsorption measurement data in optimal conditions are given in Figure 14, with the help of the Freundlich equation.

The above figure and the value of the Freundlich model correction coefficient (R^2=0.8753) show that this model has a lower agreement with the adsorption data than Langmuir. The parameters of the Freundlich model for the adsorption process of the current research are given in Table 1. The adsorption isotherm constants can be calculated by linearizing the Langmuir and Freundlich plots, as well as from the slope of the line and the width from the origin of the plot, and fitting it to the Langmuir and Freundlich equations as shown in the table below. Due to the high accuracy of fitting the data to the Langmuir model, the surface adsorption balance of the current research follows the Langmuir model. Based on this, regarding the synthesized adsorbent, it can be said that there is a fixed number of available sites on the surface of the adsorbent with the same energy level. The theoretical maximum adsorption capacity of the adsorbent is 125 mg of copper per gram of

adsorbent, which is close to the maximum adsorption capacity of the adsorbent in the real state (118 mg of copper per gram of adsorbent).

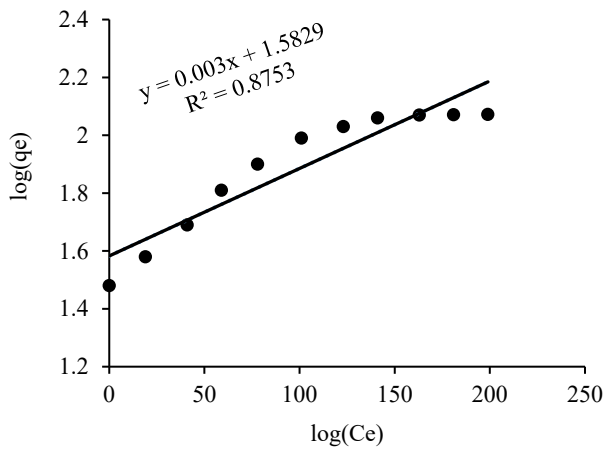

Fig. 14. Freundlich isotherm for copper ion adsorption by the m-GO@Tryp adsorbent

Table 1. Isotherm parameters of the adsorption process of the present research.

Amount	Parameter	Isotherm model
0.16	K_L	Langmuir
125	q_{max}	
0.9078	R^2	
38.27	K_F	Frendlich
33	n	
0.8753	R^2	

3.5. Investigating the thermodynamics of the adsorption process

Thermodynamic parameters are calculated using the Van 't Hoff relations [16]:

$$ln\, K_d = \frac{\Delta S_{ads}}{R} - \frac{\Delta H_{ads}}{RT} \quad (5)$$

$$\Delta G_{ads} = \Delta H_{ads} - T\Delta S_{ads} \quad (6)$$

In the above relationship, the distribution coefficient is equal to $K_d = \frac{q_e}{C_e}$, the constant amount of gases is (R=8.314 J / mol.K), and the temperature is T(K). In order to calculate the entropy of adsorption ΔS_{ads} and entropy of adsorption ΔH_{ads}, the curve $\ln K_d$ was drawn in terms of $\frac{1}{T}$ in Figure 15, and the values of enthalpy and entropy of adsorption are determined, the results are shown in Table 2.

The value of ΔG_{ads} is calculated parametrically due to its dependence on temperature with the help of Equation 6 and by substituting enthalpy and entropy in it (Table 2).

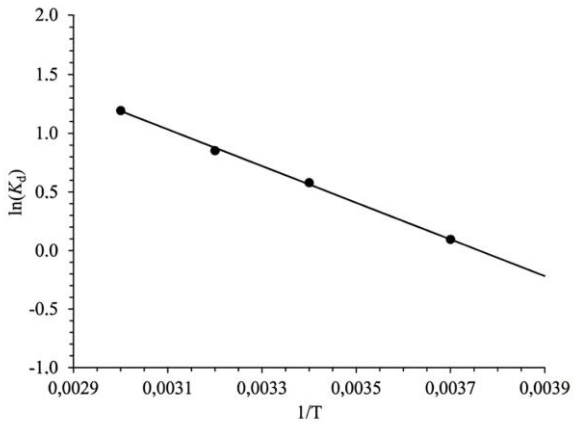

Fig. 15. Drawing of Vanthoff's thermodynamic model for the surface adsorption of copper ions with the m-GO@Tryp adsorbent.

Table 2. Thermodynamic parameters of adsorption process.

Amount	Parameter	
21.43	ΔH_{ads} $(Kj.mol^{-1})$	van 't Hoff
ΔG_{ads}=21.43-80T	$\Delta G_{ads}(Kj.mol^{-1})$	
80	$\Delta S_{ads}(Kj.mol^{-1}.K^{-1})$	

Considering the positive and relatively high value of ΔH_{ads}, it can be seen that the adsorbent has a good tendency to adsorb copper, and the adsorption reaction is endothermic.

The positive value of ΔS_{ads} also indicates the increase of disorder during the adsorption process. Due to the high value of the product of the entropy change at temperature in Equation 6, the value of ΔG is always negative.

Negative values in ΔG also indicate the spontaneity of the adsorption process.

3.6. nvestigating the adsorption process in laboratory and real wastewater samples

In order to investigate the adsorption process, two wastewater samples were prepared.

The laboratory wastewater sample consisted of a pure water solution containing copper with a concentration of 80 ppm; in addition to copper, the real wastewater sample contained lead, cadmium, and sodium chloride with a concentration of 80 ppm relative to each, which was used to check the selectivity of the adsorbent.

After removing copper and reading the concentration of the remaining solution, the efficiency of the adsorption process was checked. The results of the removal are given in Table 3.

Table 3. Copper removal rate in the wastewater sample

Sample	C_0 (ppm)	Removal (%)
Contains only copper ions	80	65
Contains copper ion, cation and electrolyte	80	46

The results in Table 3 show that the amount of copper ion removal from the laboratory sample is 65%, and from the real sample is 46%.

The removal of copper ion is reduced in the presence of other cations and electrolytes due to the selectivity of the adsorbent and its earlier saturation. The use of coagulants and coagulant aids (polyelectrolytes) can be effective in increasing the selectivity and adsorption of copper ions [20].

4. Conclusion

The nanostructure synthesized in this research showed a good adsorption effect for divalent copper cation.

The reason for this is the presence of the tryptophan nitrogen group on the surface of the nanostructure, which provides this type of adsorbent with a high adsorption capacity. The optimal pH value for copper ion adsorption was 5, and the optimal contact time was 60 minutes. An adsorbent amount of 0.1 g was selected as the optimum dose. Considering the upward trend of the temperature curve in terms of the amount of removal, it was concluded that the adsorption process is endothermic.

The adsorbent could be used only after one regeneration; after that, it could not be recovered by the acid washing method. Adsorption isotherm studies were performed using the Langmuir and Freundlich models.

The higher value of the correction factor (R^2=0.9078) in the Langmuir isotherm model showed better agreement with the data of the adsorption process compared to the Freundlich isotherm model with the correction factor (R^2=0.8753).

In fact, the higher the correction coefficient obtained through the plotting indicates a greater fit of the data to the desired model. The theoretical maximum adsorption capacity of the adsorbent was 125 mg of copper per gram of adsorbent, which was close to the maximum adsorption capacity of the adsorbent in the real state (118 mg of copper per gram of adsorbent). In order to investigate the thermodynamics of adsorption, the effects of temperature on the adsorption process were investigated using the Van't Hoff equations. The ascending curve of ΔG_{ads} with respect to temperature indicated that the adsorption process is not spontaneous.

From the positive and relatively high value of ΔH_{ads}, it can be seen that the adsorbent has a good tendency to adsorb copper, and the adsorption reaction is endothermic.

The positive value of ΔS_{ads} also indicates the increase of irregularity during the adsorption process.

The amount of removal of copper ion from the laboratory sample was 65%, while the real sample was 46%. This occurred because the removal of copper ions is reduced in the presence of other cations and electrolytes due to the selectivity of the adsorbent and its earlier saturation.

Author's contribution

All parts of this article, including conceptualization, writing, analysis, editing, and final preparation, were independently carried out by the author, Iman Khansha. The author has read and approved the final version of the manuscript.

Conflict of interest

No potential conflict of interest was reported by the authors.

Data availability

The data supporting the findings of this study are presented within the article through figures, graphs, and tables.

Funding

Self-funded.

References

[1] Yang, Q., Li, Z., Lu, X., et al. (2018). A review of soil heavy metal pollution from industrial and agricultural regions in China: Pollution and risk assessment. *Science of the Total Environment, 642*, 690–700.

[2] Jacob, J. M., Karthik, C., Saratale, R. G., et al. (2018). Biological approaches to tackle heavy metal pollution: A survey of literature. *Journal of Environmental Management, 217*, 56–70. https://doi.org/10.1016/j.jenvman.2018.03.077

[3] Akito, M., Shinichiro, Y., Akihiro, H., et al. (2014). Reevaluation of Minamata Bay, 25 years after the dredging of mercury-polluted sediments. *Marine Pollution Bulletin, 89*, 112–120. https://doi.org/10.1016/j.marpolbul.2014.10.019

[4] Dobaradaran, S., Soleimani, F., Nabipour, I., et al. (2018). Heavy metal levels of ballast waters in commercial ships entering Bushehr port along the Persian Gulf. *Marine Pollution Bulletin, 126*, 74–76. https://doi.org/10.1016/j.marpolbul.2017.10.094

[5] Peng, W., Li, H., Liu, Y., & Song, S. (2017). A review on heavy metal ions adsorption from water by graphene oxide and its composites. *Journal of Molecular Liquids, 230*, 496–504. https://doi.org/10.1016/j.molliq.2017.01.064

[6] Jamaly, S., Darwish, N. N., Ahmed, I., & Hasan, S. W. (2014). A short review on reverse osmosis pretreatment technologies. *Desalination, 354*, 30–38. https://doi.org/10.1016/j.desal.2014.09.017

[7] Kim, B. K., Lee, E. J., Kang, Y., & Lee, J. J. (2018). Application of ionic liquids for metal dissolution and extraction. *Journal of Industrial and Engineering Chemistry, 61*, 388–397. https://doi.org/10.1016/j.jiec.2017.12.038

[8] Hao, J., Ji, L., Li, C., et al. (2018). Rapid, efficient and economic removal of organic dyes and heavy metals from wastewater by zinc-induced in-situ reduction and precipitation of graphene oxide. *Journal of the Taiwan Institute of Chemical Engineers, 88*, 137–145. https://doi.org/10.1016/j.jtice.2018.03.045

[9] Luo, T., Abdu, S., & Wessling, M. (2018). Selectivity of ion exchange membranes: A review. *Journal of Membrane Science, 555*, 429–454. https://doi.org/10.1016/j.memsci.2018.03.051

[10] Bansod, B. K., Kumar, T., Thakur, R., et al. (2017). A review on various electrochemical techniques for heavy metal ions detection with different sensing platforms. *Biosensors and Bioelectronics, 94*, 443–455. https://doi.org/10.1016/j.bios.2017.03.031

[11] Akhlaghian, F., Ghadermazi, M., & Chenarani, B. (2014). Removal of phenolic compounds by adsorption on nano structured aluminosilicates. *Journal of Environmental Chemical Engineering, 2*, 543–549. https://doi.org/10.1016/j.jece.2013.10.009

[12] Wanjeri, V. W. O., Sheppard, C. J., Prinsloo, A. R. E., et al. (2018). Isotherm and kinetic investigations on the adsorption of organophosphorus pesticides on graphene oxide based silica coated magnetic nanoparticles functionalized with 2-phenylethylamine. *Journal of Environmental Chemical Engineering, 6*, 1333–1346. https://doi.org/10.1016/j.jece.2018.01.064

[13] Bhattacharyya, S., Raju, R. U. R., & Kumar, P. (2025). Graphene-based nanomaterials for wastewater treatment – A review on advances, optimization, and future perspectives. *Progress in Engineering Science, 2*(3). https://doi.org/10.1016/j.pes.2025.100107

[14] Tee, et al. (2024). A high-performance 3D phosphorus-doped graphene oxide adsorbent for imipramine wastewater treatment. *Separation and Purification Technology, 330*. https://doi.org/10.1016/j.seppur.2023.125266

[15] Meymane Jahromi, H., & Khonsha, I. (2022). Tryptophan-modified magnetic graphene oxide for adsorption of copper(II) cation. *Chemical Research in Nanomaterials, (1)*, 47–55.

[16] Vimlesh, C., Jaesung, P., Young, C., et al. (2010). Water-dispersible magnetite-reduced graphene oxide composites for arsenic removal. *ACS Nano, 4*, 3979–3986.

[17] Teymourian, H., Salimi, A., & Khezrian, S. (2013). Fe3O4 magnetic nanoparticles/reduced graphene oxide nanosheets as a novel electrochemical and bioelectrochemical sensing platform. *Biosensors and Bioelectronics, 49*, 1–8. https://doi.org/10.1016/j.bios.2013.04.034

[18] Khonsha, I., Heidarinasab, A., Moniri, E., & Ahmadpanahi, H. (2017). Removal of hexavalent chromium in industrial wastewater using poly[allylamine-(N,N-dimethylacrylamide)] grafted onto magnetic nanoparticles. *Advances in Polymer Technology, 36*, 371–377. https://doi.org/10.1002/adv.21618

[19] Ahmad Panahi, H., Morshedian, J., Mehmandost, N., et al. (2010). Grafting of poly[1-(N,N-bis-carboxymethyl)amino-3-allylglycerol-co-dimethylacrylamide] copolymer onto siliceous support for preconcentration and determination of lead (II) in human plasma and environmental samples. *Journal of Chromatography A, 1217*, 5165–5172. https://doi.org/10.1016/j.chroma.2010.06.012

[20] Amiri, M. C. (2006). *Principles of water treatment*. Arkan Publication.

How to cite this paper:

Khonsha,I. (2026). Removal of copper (II) ion by functionalized graphene oxide nano adsorbent from wastewater sample. *Advances in Environmental Technology*, 12(3),407-419. DOI: 10.22104/aet.2026.7599.2132